Desalination and Water Treatment
www.deswater.com
doi: 10.5004/dwt.2020.26272

204 (2020) 22–32
November

The commissioning of absorption heat transformer for water distillation using solar panels

S.G. Perez[a], A. Huicochea[b], G. Urquiza[b], A.H. Hernández[c], J. Siqueiros[d,*]

[a]*Posgrado del Centro de Investigación en Ingeniería y Ciencias Aplicadas (CIICAp) de la Universidad Autónoma del Estado de Morelos (UAEM), Av. Universidad No. 1001, Col Chamilpa, CP.62209, Cuernavaca, Morelos, México, Tel. +52 01 777 3297084; email: sandro.perez@uaem.mx (S.G. Perez)*
[b]*CIICAp-UAEM, emails: huico_chea@uaem.mx (A. Huicochea), gurquiza@uaem.mx (G. Urquiza)*
[c]*Universidad Politécnica de Atlautla (UPAtlautla). Carretera Atlautla-Ozumba No. 12, Barrio San Jacinto C.P.56970, Atlautla, Estado de México, México, email: angel_hernadez@upatlautla.edu.mx (A.H. Hernández)*
[d]*Consejo de Ciencia y Tecnología del Estado de Morelos, Av. Atlacomulco No. 13, Colonia Acapatzingo, C.P. 62440, Cuernavaca, Morelos, México, email: jsiqueiros@uaem.mx (J. Siqueiros)*

Received 12 July 2018; Accepted 16 June 2020

ABSTRACT

A solar collector system is coupled to an absorption heat transformer to distill water, using a Carrol/water working solution of 63% by weight in the generator (Carrol is a mixture of lithium bromide and ethylene glycol). The system has two collector blocks connected in series with an approximate inclination of 18° and south orientation five solar panels parallel connected, measuring 1.85 m × 1.10 m, and two solar panels with 2.05 m × 0.93 m, with a total area of 14 m^2. The maximum efficiency of the solar panels is 0.75, and the power 10.79 kW. The solar energy is supplied heat to the generator to increase the coefficient of performance of the absorption heat transformer up to 0.78.

Keywords: Water distillation; Solar panels; Absorption heat transformer

1. Introduction

1.1. Energy situation

Solar radiation is the most important source of renewable energy on earth; it is inexhaustible, abundant and free. Our planet receives this energy in the atmosphere and exceeds the annual population requirements worldwide. Solar energy that falls by 1 m^2 could save approximately 100 L of gasoline in 1 y [1]. In today's industrial societies, the scarcity of fossil fuels and their adverse effects on global warming and air pollution are cause for immediate attention. In addition, there are many thermal systems that release large amounts of residual heat at low temperatures of 60°C–100°C to the environment [2].

1.2. Solar technology

Solar thermal energy today, despite the recent boom in photovoltaic energy, represents the largest solar contribution to our energy needs, with more than 196 gigawatts of thermal capacity and 162 terawatts thermal hour produced in 2010 [3]. There are different technologies to capture solar energy, a solar panel (SP) is a technology that extracts part of the heat produced by the downward flow of solar radiation and becomes a source of energy. The outstanding elements among the most advantageous and low manufacturing and maintenance costs for businesses such as food, beverages, textiles, metallurgical, surface treatment, paper and, chemical industry; where hot water is wasted in the process or where there is high and continuous employment

* Corresponding author.

of energy SP energy can be used when the heat is required from a clean energy source with thermal levels ranging between 60°C and 280°C, and up to 400°C for electricity generation systems [4]. Another technology is the tubes evacuated to capture solar energy are suitable for low-temperature applications (180°C–300°C), due to the high coefficient of thermal loss [5]. Empirical studies were carried out with a heat pump coupled to a floor with a SP system, connected in a row, to heat a room. This work was presented at a solar heating plant in China; the use of SP energy is suggested as an alternative source for the heat pump, instead of recharge wells, for heat storage. It was concluded that the process of solar-assisted heating has a significant effect on the improvement of the well temperature and energy efficiency, which confirmed that the heat pump together with a plant with SP system will be more convenient for heating the rooms in cold areas [6]. Ayompe and Duffy [7] analyzed the thermal behavior of a solar water heating system with an SP in a cold zone in Dublin, Ireland. The maximum temperature of the fluid when leaving the registered collector was 70.4°C, SP efficiency of 45.6% and system efficiency of 37.8%. The losses shown in the supply tube were 16.4% of the energy collected. They concluded that since the total annual heat loss in the pipes for the supply was 1,171.7 MJ, which is equivalent to 16.4% of the energy collected and 19.8% of the energy delivered to the hot water tank. Supply pipes should be kept as short as possible to reduce energy loss. They analyzed a SP from the point of view of exergy where the SP was operated with single-wall carbon nanofluids as an absorbent medium. Nanofluids reduce the generation of entropy by 4.34% and increase the heat transfer coefficient by 15.33% compared to water as an absorbent fluid [8]. They experimented with an SP where the working fluid was SiO_2/ethylene glycol. The thermal efficiency and performance characteristics of the SP are obtained for mass flow rates between 0.018 and 0.045 kg/s. The characteristics of the solar collector curve indicate that the effects of particle loading in improving thermal efficiency are more relevant in the higher values of the heat loss parameter. SiO_2 nanoparticles improve the efficiency of SPs despite their low thermal conductivity compared to other usual nanoparticles [9].

1.3. Absorption heat transformer

To reduce fuel consumption and environmental pollution, the heat absorption transformer (AHT) is used, which is activated with residual heat or a renewable energy source (solar or geothermal). An AHT is capable of purifying water and saves energy without contamination [10]. An AHT uses energy with a low thermal level (from 60°C to 80°C) and increases it to a higher thermal level (90°C–120°C). Energy from the SP can be used to activate its thermodynamic cycle. Its main advantages are: it does not pollute, it can use energy that does not come from fossil fuels, it has a closed cycle and it produces high-quality energy for the process that needs it, such as pasteurization, desalination, sterilization, air conditioning, steam production, roasting, drying and purification [11,12]. The most commonly used working solution in AHT is lithium bromide-water, however, it has the disadvantage of crystallization at concentrations close to 70% by weight. Another working solution is Carrol/water, where Carrol is a mixture of lithium bromide [LiBr] and ethylene glycol [$(CH_2OH)_2$] in the ratio 1:4.5 by weight (Carrier Corporation, Florida Beach Gardens, Florida, U.S.A.). This mixture has thermodynamic characteristics similar to that of lithium bromide-water with high solubility of up to 80% by weight, which makes it possible to operate the heating system at higher temperatures with less corrosion problems, in addition, the working solution selection is a critical part for the proper functioning of the AHT since the cycle develops according to the thermodynamic, chemical and physical properties of the working solution (absorbent and refrigerant). So a study was made at AHT using Carrol water at 59%, 63% and 70% as a working solution. The best results of the energy coefficient of performance (COP) were achieved with the working solution of 63% because it's thermodynamic and transport properties were optimal for the desorption and absorption processes Torres [13]. Condensation temperatures and the effectiveness of solution heat exchangers have been shown to favor crystallization [14]. The basic AHT reaches low gross temperature lift (GTL) with respect to a double absorption AHT [15]. A mathematical model was proposed to optimize the thermodynamic performance of an AHT, where it was shown that energy efficiency and exergy could increase by 10% and 5.3%, respectively in the most optimal condition [16]. An experimental analysis of an AHT was performed under controlled conditions with the $H_2O/LiCl/ZnCl_2$ and $H_2O/CaCl_2/ZnCl_2$ working solutions, where the performance of a solar absorption system for simultaneous cooling and heating operating with H_2O/LiBr and alternative mixtures of aqueous hydroxide (NaOH:KOH:CsOH). The system with the hydroxide mixture can operate with higher performance coefficients than the system with the lithium bromide mixture and with a higher temperature range [17]. A method to evaluate the characteristics and performance of a single-stage H_2O/LiBr absorption machine was presented with the mass and heat transfer equations. The analysis showed that the greater the difference between the input and output concentrations of LiBr in the absorber is lower the mass circulating in the absorber [18].

1.4. Solar panel – absorption heat transformer

The experimental coupling of SP to AHT is very limited. The AHT has been used to improve the thermal level of a solar pond, since the GTL was 44°C with a COP between 0.10 and 0.16 [19]. The temperature of a solar pond for water desalination at 100°C can be reached by means of an AHT. To obtain 1 m^3 of desalinated water in 1 d, a solar pond between 1,000 and 4,000 m^2 is needed [20]. A theoretical proposal is to use a flat plate collector to supply the activation heat in a solar double stage absorption heat transformer, which works with the H_2O-LiBr solution. The results show that there is an optimum temperature of the absorber/evaporator to obtain the minimum values of CPK (capital cost per kilowatt of heat capacity) and PP (recovery period). It is possible to obtain minimum values CPK of 928.1 euros/kW and PP of 4.0 y respectively at absorber/evaporator of 104°C, with a solar radiation intensity of 600 W/m^2, generation temperature at 75°C, condensation temperature at 38°C, absorption temperature at 135°C and economizer efficiency adjusted to 0.8 [21].

After conducting a review of the literature, no work was found in which an experimental absorption heat transformer for water distillation is activated through the use of solar panels. There are several theoretical and experimental studies focused on the individual study of AHT and SP respectively, where the main objectives have been focused on improving the performance of energy through new configurations, heat and mass transfer coefficient, heat transfer areas, falling film and pool boiling, new heat exchangers, etc.

On the other hand, renewable energy sources must be used as much as possible to mitigate pollution and conserve fossil reserves, since environmental conditions for living beings are more aggressive to their health. Based on the above, this experimental work studies the use of solar energy to active the thermodynamic cycle of an AHT. Solar energy is supplied to the generator to reduce the heat demand of the AHT, and therefore improve the COP. The performance of the SP-AHT, the behavior of the generator and the amount of distilled water is analyzed considering different environmental conditions.

2. Description of the solar panel

Fig. 1 shows the SP system. This is a Max-Solar C/Hipertinox (AXOL-Hiper-Tinox model), manufactured by the Modulo Solar Company (Cuernavaca, Morelos, México). The system has two blocks of solar panels that are connected in a row, with an approximate tilt of 18° and facing south: five solar panels with a parallel connection, measuring 1.85 m × 1.10 m and two solar panels in a row, measuring 2.05 m × 0.93 m, with a total surface of 14 m^2. The first block (1, 2, 3, 4, 5) serves to increase the heat received, and the second block (6, 7) serves to increase the fluid temperature to meet the requirements of the AHT generator for purifying water. All they are connected by a copper pipe with a diameter of 2.54 cm. Inside, they have 9 copper fins with a diameter of 0.635 cm per panel; they have a black enamel coating as a heat absorbent. The panel's lining is made of 1.27 cm of polyurethane, as thermal insulation, and it has a 4 mm transparent glass cover to increase solar energy collection.

The water storage tank is cylindrical, made of carbon steel with an epoxy coating. External measurements are 1.722 m long and 0.608 m in diameter, with a capacity of 500 L. It includes insulation with a side exit of 2.54 cm in diameter and a polyurethane cover which is 3.81 cm wide, used for thermal insulation. Interconnection tubing is 2.54 cm in diameter. It uses a 0.745 kW Grundfos pump (Manufactured in Bjerringbro, Denmark), which is automated by a differential temperature controller (with two sensors) and panels with a pressure release valve. This valve works at 1.034 MPa and 100°C, avoiding the build-up of pressure and temperature; there is also a ventilation valve. According to the technical specifications of the provider, the SP system may reach temperatures of up to 80°C, for which it may be used as activation heat in AHT components. The capacity of the solar system was previously determined by considering the energy requirement of the AHT based on previous experimental tests shown in Table 1, where the heat needed to reach saturation conditions in the generator for 7 h was 1.44 kW at 90.4°C maximum. The array of 7 solar collectors (series and parallel) and a 500 L water tank meet the generator demand of the AHT.

2.1. Description of absorption heat transformer for distilled water

Fig. 2 shows the configuration of the Absorption heat transformer to distilled water (AHTDW). It is composed of the main circuit and three secondary circuits. The main circuit components are generator, condenser, evaporator, absorber and economizer. These components are heat exchangers, made of stainless steel 316 L. The generator and the absorber are formed by the casing and tubing; the rest are spiral exchangers with a central pipe. The generator concentrates the water Carrol working solution to 63% by weight. This process takes place under certain saturation conditions (pressure and temperature) where part of the working fluid is separated from the working solution. The

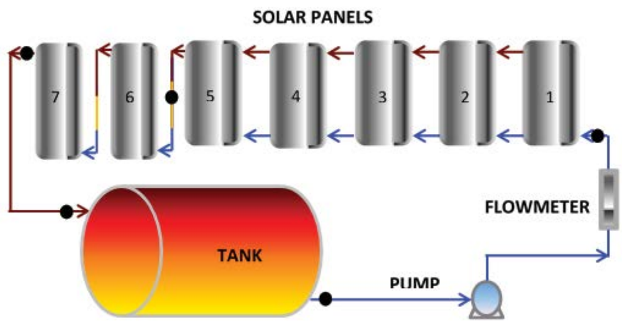

Fig. 1. Solar panel system.

Table 1
Previous work to determine the capacity of the solar system

Works	Author	Generator inlet temperature (°C)	Heating mass flow (L/min)	Test time (h)	Generator heat (kW)
Experimental study of a water purification system coupled to an AHT using the water/Carrol mixture	Hernández Soria [22]	90.07	6–7	7	0.24–1.44
Experimental evaluation of a thermal transformer using water/Carrol	Torres [13]	90.4	6.8	4.75	0.64
Theoretical and experimental study of a system for water purification integrated into a thermal heat transformer using water/Carrol	Huicochea [12]	78.0–90.6	0.13	4	0.61–1.06

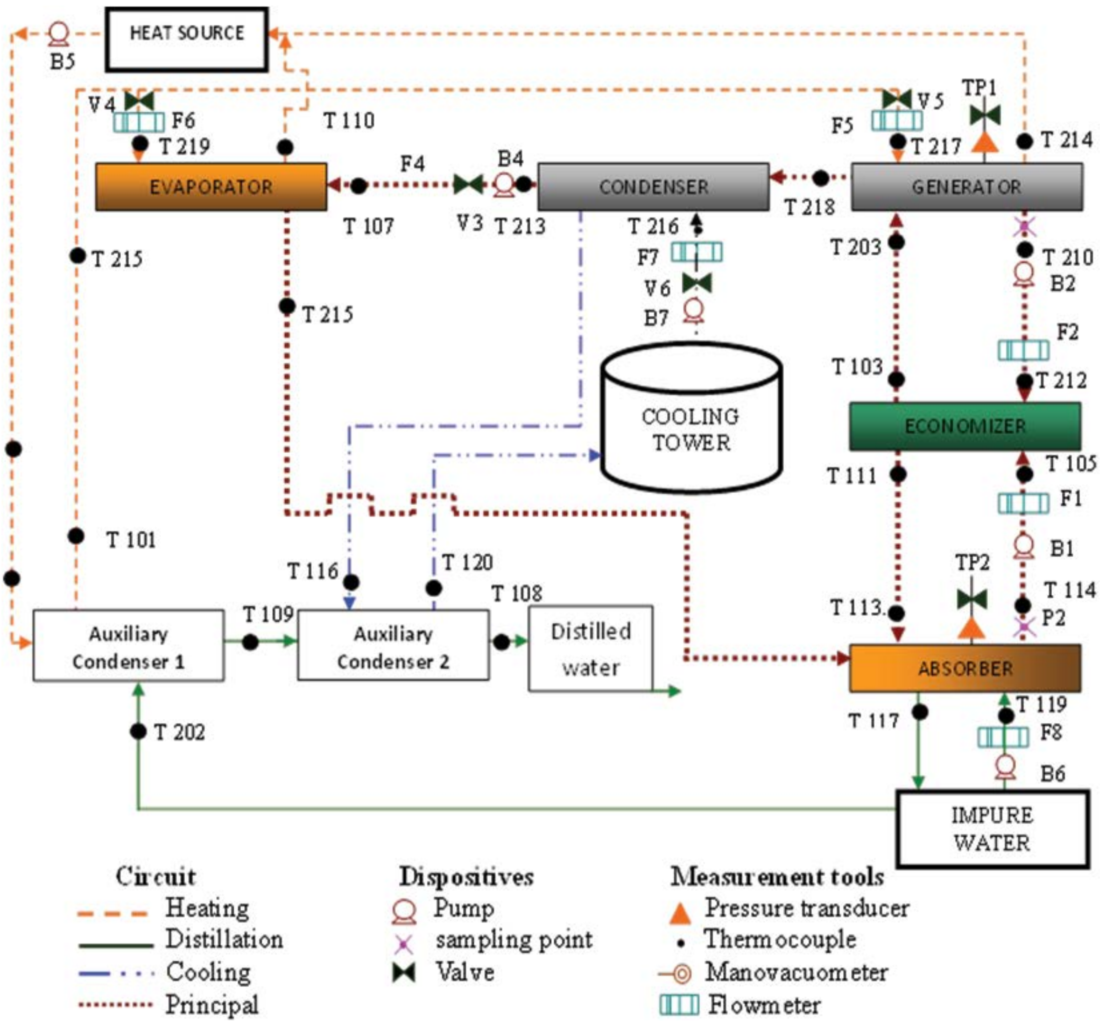

Fig. 2. Configuration of AHTDW.

generator's working fluid flows to the condenser, whose function is to change the phase of the working fluid from vapor to sub-cooling liquid. This liquid moves towards the evaporator, whose function is to change the phase of the working fluid from liquid to overheated vapor. This vapor and the working solution coming from the generator are mixed in the absorber, which releases useful heat at a higher thermal level than the one which was delivered (to the generator and evaporator), through an exothermic reaction. The economizer pre-heats the concentrated solution working that flows from the generator to the absorber, using the energy of the solution working that flows from the absorber to the generator. In this experimental analysis, a water Carrol solution at 63% weight was used, since the literature reports maximum COPs of 0.34 and 0.28 at the same concentration [12,22].

2.2. Coupling of SP system with the AHTDW

Fig. 3 shows the coupling of the SP system and the AHTDW. In this work, two non-polluting technologies are joined. The SP system has the following advantages: low cost, basic manufacturing, extended commercial distribution, low maintenance cost, and dependability. It obtains thermal power at a maximum temperature of 80°C reported by Modulo Solar Company in Cuernavaca, Morelos, México. This technology is an environmentally friendly alternative because it uses energy that does not come from fossil fuels; it also has a closed cycle. This means that the working solution is not used up nor does it pollute because it has no contact with the outside environment while generating high-quality power for processes that require temperatures between 80°C–120°C. In the task described in this work, it was used to distilled water by using an AHT.

Table 2, an investigation was carried out of the types of solar panels existing in the local market with their thermodynamic and transport characteristics, as well as their costs. It is determined that flat-plate solar collectors are a viable option because of temperature and cost.

3. Method

The SP system begins to function at early hours, in order to collect the greatest amount of solar power. When

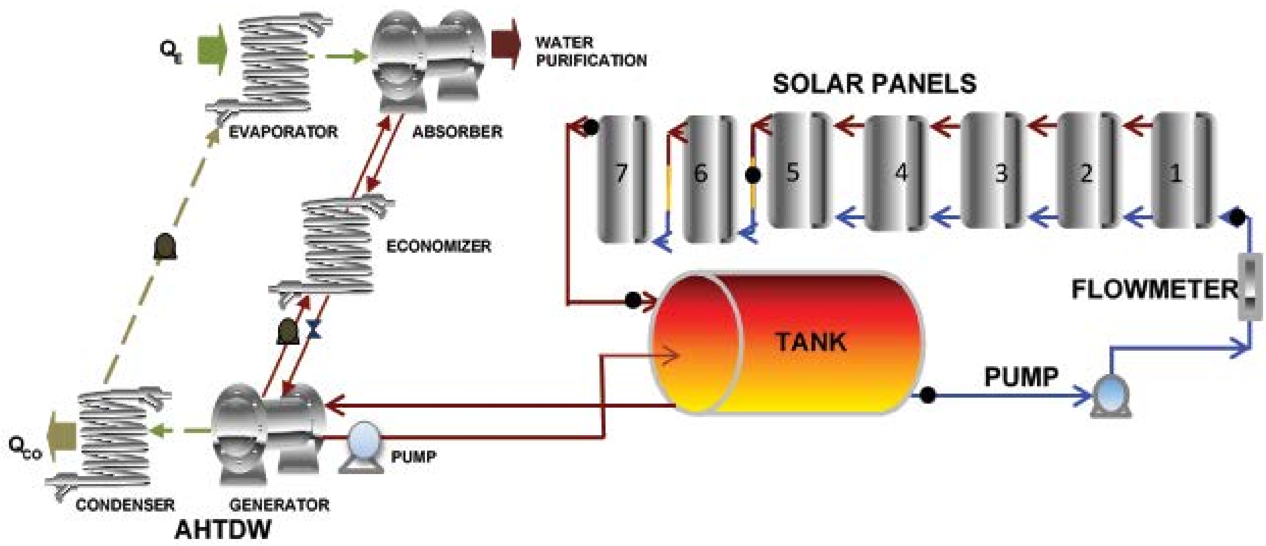

Fig. 3. Coupling SP system with the AHTDW.

Table 2
Comparison of solar panels

Types	Operating temperature (°C)	Cost per unit
Flat solar collector	≤82	$6,363
Flat solar collector with reflecting surface	60–120	$8,321
Vacuum tubes collector	100–200	$11,356
Parabolic segment concentration sensor	80–200	$241,000

the refrigerant of the SP system reaches 42°C, the AHT is turned on; this is at the minimal absolute pressure, in order to reach the saturation conditions of the working solution at a low temperature in the generator. Once the maximum solar radiation has been reached, heat is provided to the generator, to obtain vapor. The methodology was as follows: water flows through the copper tubing, which is in contact with the solar radiation absorbing plate and is pumped to a carbon steel storage tank which is insulated by a 1½″ polyurethane cover. The configuration consists of three parts of the SP system: in series, in parallel and a third that is achieved by coupling the other two. Like this, the SP system is coupled to the AHT to reach an adequate temperature and be able to send the liquid to the entrance of the generator. The SP system was tested during 9 months (January to September), from 8 a.m. to 5 p.m. To measure the heat fluids supplied to the generator, a fluxmeter was used with a maximum measured flux of 15 L/min, with 3% precision in the measurement of the total relationship. To measure temperature in the SP system, *T*-type thermocouples were used with ±0.1°C of accuracy, which resulted in ±0.2°C uncertainty for each thermocouple pair. For data acquisition, a data logger from Agilent Technologies (Manufactured in Santa Clara, California, U.S.A.) was used, 34970A series with 20 channels of voltage access for the direct measurement of the thermocouples. The process included the start-up of the SP system, knowing its thermal levels, period and duration, coupling the systems and starting tests by making hot water coming from the SP flow through the storage tank towards the AHTDW generator in order to transfer energy; then, making the water flow again towards the SP system to increase its thermal level and repeat the cycle in such a way that it is synchronous with the AHTDW. The circuits are then activated, where the generator will take that energy in order to increase its thermal level and get saturation conditions in the solution which are needed to reach the stable state (without changes), thus obtaining distilled water in the AHTDW.

3.1. Calculation of components in the system of SP

The yield of the collector is defined as the relationship between collected energy and energy received at a given point in time. Eqs. (1) and (2) include the mass flow, input and output water temperatures, as well as the water's C_p at a different temperature.

$$\eta = \frac{Q_u}{S} \cdot I \tag{1}$$

Replacing Q_u by its value, in the Bliss equation [23], leads to:

$$\eta = F_R \cdot (\tau \cdot \alpha)_N - F_R \cdot U \cdot \left[\frac{\left(T_M^0 - T_a^0\right)}{I} \right] \tag{2}$$

3.2. Calculation of uncertainty for coupling

The combined uncertainty was obtained through the Taylor series method [24], where "y" is given by a model, $y = f(x_1, x_2, x_N)$, the combined $U_c(y)$ uncertainty is given by $U_C^2(y) = \sum_{i=1}^{N} \left(\frac{\partial f}{\partial x_i} \right)^2 U^2(x_i)$, which was used to determine the combined uncertainty in the direct and indirect variables of the SP-AHT coupling. Table 3 shows the main uncertainties.

3.3. Comparison of thermal desalination technologies

Different technologies exist for thermal desalination where there is a large economic and technical investment [25,26]. An alternative is the one developed in this work, where simple-effect evaporation is achieved by taking advantage of the useful heat obtained in the AHT, which uses solar heat. Table 4 shows a comparison of the proposals reported up to now, using different thermal technologies.

3.4. Calculation of components of AHTDW

External balance for the evaluation of the AHTDW, starting with energy equilibrium and based on the principle of energy conservation [27], proves that:

$$Q_{EV} + Q_{GE} = Q_{AB} + Q_{CO} \quad (3)$$

Calculation of the input power: generator and evaporator:

$$Q_{GE} = (\dot{m}_{GE})(\Delta h) \quad (4)$$

$$Q_{EV} = (\dot{m}_{EV})\ (\Delta h) \quad (5)$$

Calculation of output power: absorber and condenser.

$$Q_{AB} = (\dot{m}_{AB})\ (\Delta h) \quad (6)$$

$$Q_{CO} = (\dot{m}_{CO})\ (\Delta h) \quad (7)$$

Using the power data, the COP is calculated; this is the most important parameter in a heat transformer. It is defined as the power provided by the absorber Q_{AB} divided by the total amount of power provided to the generator and the evaporator ($Q_{GE} + Q_{EV}$) [28]:

$$\text{COP} = \left(\frac{Q_{AB}}{Q_{GE} + Q_{EV}} \right) \quad (8)$$

The work of the positive displacement pumps is ignored, since the high-quality energy used is very low, compared to the thermal energy provided to the equipment [27,29].

In this work, in order to make the coupled systems more effective, to present a COP of the AHTDW coupled to the SP system (COP_{SP}), which is the result of the energy obtained in the absorber divided by the energy in the evaporator because the energy in the generator is supplied by renewable energy.

$$\text{COP}_{SP} = \left(\frac{Q_{AB}}{Q_{EV}} \right) \quad (9)$$

Table 3
Uncertainty of the main components

Solar panels	
Variables	Uncertainty (%)
T_{out} hot water	±0.2
$\dot{m}_{ac}$	±0.03
Q_u	±5.02
Absorption heat transformer	
Q_{GE}	±14.13
$T_{out,GE}$	±0.2
COP	±15.17

4. Results

Fig. 4 shows the behavior of temperatures in the SP system during almost 11 h (May 17, 2017). At approximately 14:20 h the output temperature of the tank was over 64°C. From this point, heated water is provided to the generator; this is the minimum temperature required by the AHTDW to initial the operation. The temperature increases to over 65°C at 14:50 h and it remains, for about 4 h (until 17:50), because the exit temperature in the SP is greater than this temperature, reaching values of 88.9°C. During this time, an experimental test was carried out.

Table 5 shows the 4 average temperatures of water in the different points of the SP system, obtained from May 13 to 17, 2017. The maximum temperature was obtained at the SP exit; from this point, water flows to the generator in order to transfer energy.

Fig. 5 shows the behavior of solar radiation on May 17, 2017. The maximum value obtained was 932 W/m^2, when multiplied by the collector area of 14.0 m^2, reaching a total of 13.05 kW at approximately 12:10 h; this is because the sun shines directly on the SP at this hour. Radiation variations during the day are shown under the curve because some clouds covered the sun during this period and solar radiation decreased. It is good to clarify that, depending on the seasons and the day, radiation changes, and this will be reflected in the curve. There are different methods to determine solar radiation: mechanical actinograph graph, Kriging geostatistics (latitude of the site), estimated radiation (satellite image) and in situ measurement (pyranometer). The in-situ measurement method was used for our study. Solar radiation characteristics were provided by the CONAGUA meteorological station, which is near the research laboratory.

The experimental tests were developed in the spring, in order to have maximum solar radiation in the laboratory zone. The main parameter in SP efficiency is the yield curve. Fig. 6 represents the estimated yield vs. the temperatures and received solar radiation. A maximum of 0.75 efficiencies

Table 4
Comparison of thermal technologies to desalinate water

Thermal and membrane desalination processes	Installation in Mexico (%)	Energy consumption (kWh/m^3)	Cost (USD/m^3)
Multi stage flash distillation (thermal)	4%	8 kWh/m^3	1.10 USD/m^3
Multiple stage distillation (thermal)	1%	4 kWh/m^3	1.5 USD/m^3
Inverse osmosis (membrane)	50%	2.8kWh/m^3	0.6 USD/m^3
Solar-absorption heat transformer (thermal-solar)	Growing	Minimum because solar energy is used	Installation nothing more

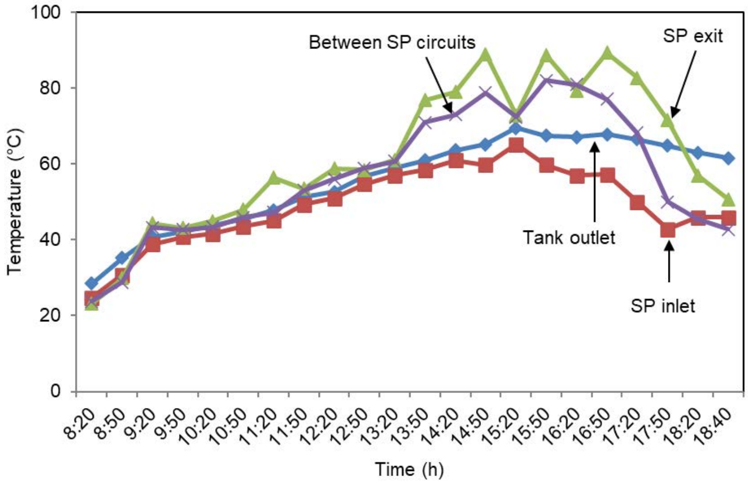

Fig. 4. The behavior of the temperature of the SP related to the time.

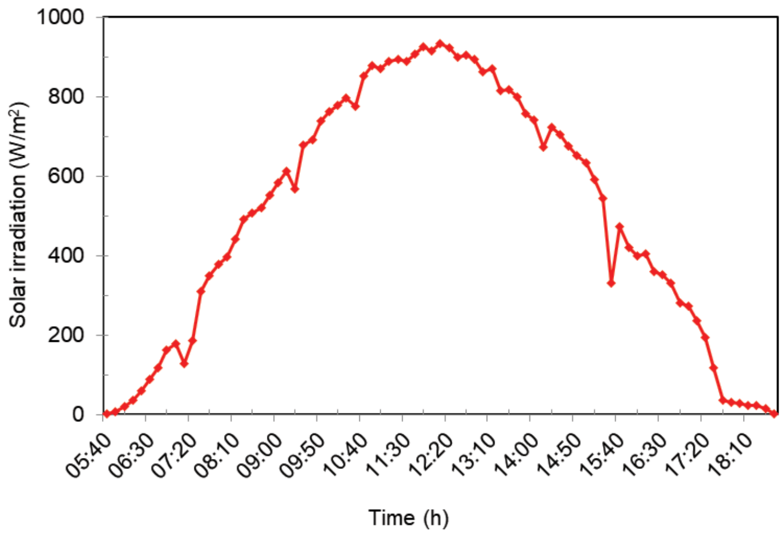

Fig. 5. Solar irradiation on May 17th.

was obtained, at an ambient temperature of 31.6°C. In the SP installation, the NOM003-ENER-2011 [30] and ANSI/ASHRAE-93-1986 [31] procedures were used to determine the efficiency. The SP specifications were gotten from the manufacturer and may be found in section 2.0.

Fig. 7 shows the energy in the generator (figured with the equation: $Q = m \times \Delta h$) and its evolution over time. The range of heat energy increases at 11:40 h, from 1.5 to 3.45 kW. The highest powers are obtained starting at 15:45 h during the test, as well as the main recorded temperatures (Fig. 4),

Table 5
Average in parameters on operation of SP

Position	Temperature at 12:00 h/d	Maximum temperature in the day	Temperature at 17:00 h/d
T_{out} of tank	47.7°C	71.0°C	67.5°C
T_{in} to SP	43.2°C	66.1°C	53.9°C
T between SP	54.5°C	84.4°C	75.6°C
T_{out} of SP	60.0°C	88.9°C	88.2°C

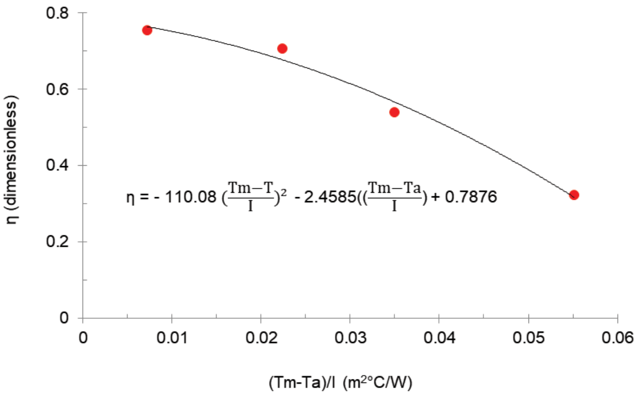

Fig. 6. The efficiency of the SP system.

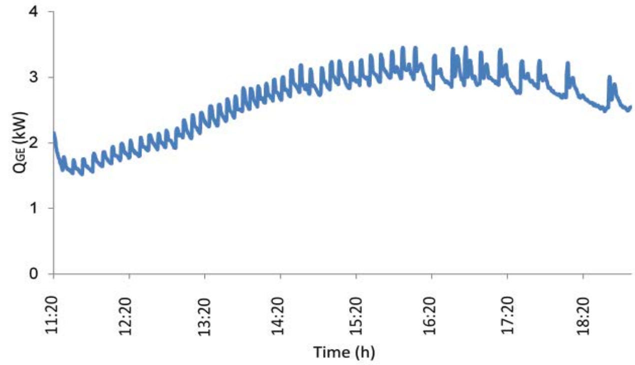

Fig. 7. Evolution in time of the calorific power in the SP system.

since these values are directly proportional. Here we need to mention that fluctuations in the figure are due to the intermittent operation of the pump. Heat flow in the generator represents the heat going through the solar panels, which is deposited in the storage tank where it supplies the generator; heat losses in the component do not affect the performance evaluation, since only the in-transit heat flow is considered.

Fig. 8 shows the AHTDW behavior in an experimental test, coupled with the SP system as a source of energy. The test began at 14:00 h with the coupling between AHT-SP systems. The temperature of the water entering the generator was approximately 78°C, and this was supplied from the storage tank, where the internal temperature was 82°C, given by the SP. The stability criterion for AHT was defined when the temperature of the absorber in the external circuit varied between 93.5°C and 94.5°C for a period of 90 min. The stable state was reached 2.5 h after having started the experimental test, where the maximum temperature in the absorber was 94.0°C with a maximum GTL of 16.9°C. The evaluation of the water purification system was carried out in the last 12 min of the stable state of the AHT by the thermal inertia of the processes connected in series, shown in Fig. 3. The water purification process at 614 mmHg demands a saturation temperature of 94.1°C, REFPROP [32]. For this experimental study, the generator's temperature does not decrease, although solar radiation decreases over time since the supply to the generator comes from the 500 L storage tank.

Fig. 9 shows the behavior of temperature and thermal energy in the generator against time. We see that input temperature to the generator, at 14:00 h was near 40°C and shows a positive slope until reaching approximately 78.9°C.

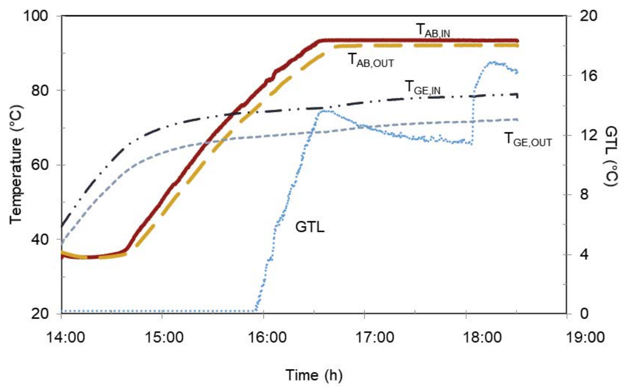

Fig. 8. Temperature vs. time of the AHTDW.

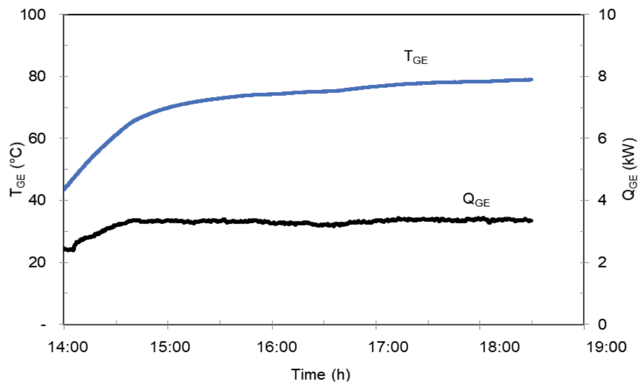

Fig. 9. The behavior in the generator of AHTDW.

After 42 min, the behavior of the energy in the generator is almost continuous, with a power of 3.45 kW.

Fig. 10 shows the behavior of 2 temperatures: one is the SP output and the other is the input temperature to the generator. The SP heat was used as an energy source for the generator, and through a thermodynamic cycle, the temperature increases up to a higher thermal level. It shows that the SP temperature at 10:00 h was 22°C, while the temperature at the entrance of the generator, without heating water flow, was 18°C. When the temperature at the SP entrance increased to 60°C, the SP system and the AHTDW were coupled.

5. Efficiency and performance

Table 6 includes the values obtained from the experimental tests. The SP's efficiency resulted from the useful power divided by the product of the radiation intensity (provided by CONAGUA) [33]. The COP is the power obtained in the absorber, divided by the energy supplied to the generator and the evaporator, while the COP_{SP} is the result of the energy obtained in the absorber divided by the energy supplied to the evaporator, not counting the energy supplied to the generator, since this was obtained from solar radiation.

Also, in Table 7 shows the energy from the generator, evaporator and absorber (Eqs. (4)–(6)). Between 70.72% and 71.31% of the energy used by the AHTDW is provided by the SP system, which is the percentage of energy for the generator.

Fig. 11a shows the COP with respect to COP_{SP}. COP_{SP} is greater because it was not divided by the power of the generator, since this energy was provided by the SP. This was different from the COP, where it is the result of the power of the absorber, divided by the sum of the powers of the generator and the evaporator. The COP_{SP}, as has been mentioned before, are directly proportional to the power of the absorber. Fig. 11b shows the behavior of the distillate obtained with respect to the COP in the experimental tests.

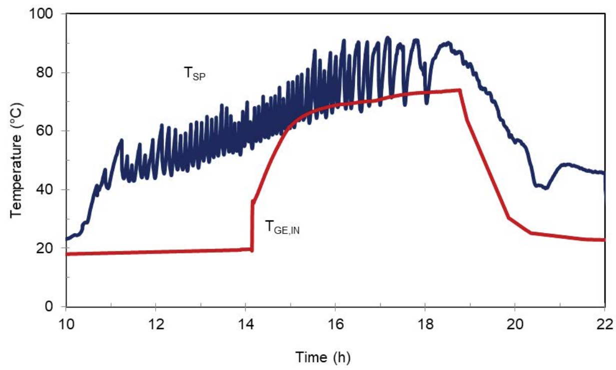

Fig. 10. Evolution in time of the SP system coupled to AHTDW.

Table 6
Efficiency of solar panels

Q_u (W)	I (W/m²)	A (m²)	η (dimensionless)
10,795	1,023	14.0	0.75
10,341	1,046	14.0	0.71
7,438	932	14.0	0.57
3,810	842	14.0	0.32

Table 7
Values of efficiencies and powers

	Maximum	Minimum
Q_{GE}	3.45 kW	3.28 kW
Q_{EV}	1.39 kW	1.36 kW
Q_{AB}	1.09 kW	0.72 kW
COP	0.22	0.15

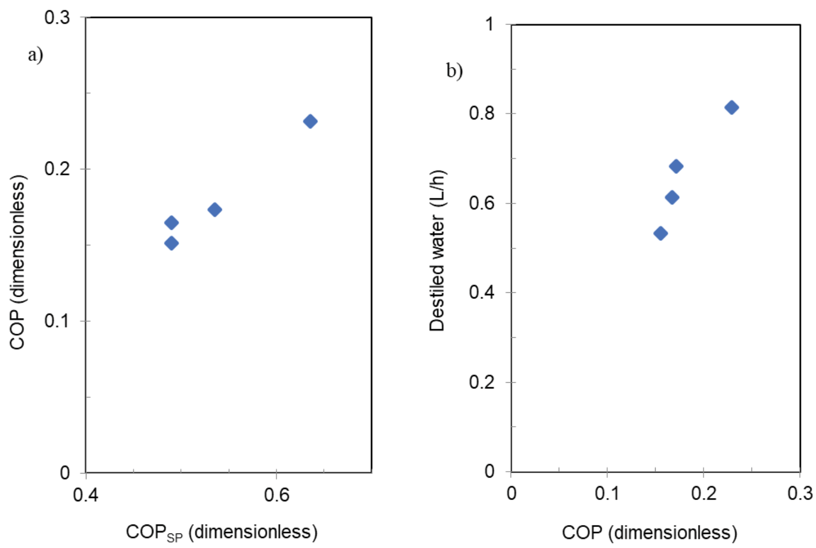

Fig. 11. (a) COP against COP_{SP} and (b) distilled water against COP.

6. Conclusions

A system of solar panels was connected to an AHTDW as a source of energy. The maximum efficiency of the solar panels was 0.75 at 12:20 h. Saturation conditions in the generator could not be maintained after 18:30 h; thus, alternative heating is needed. The solar panel system provides approximately 70% of the total energy required for the operation of the absorption heat transformer, where the coupling of the solar system is done directly to the generator and the maximum temperature reached in the SP was 88.9°C. The AHTDW used the water Carrol working solution at a Carrol concentration of 63% by weight, where the temperature in the absorber was 94°C, GTL was 16.95°C and 0.01 L/min of distilled water were obtained.

Abbreviations and symbols

AB	—	Absorber
AHTDW	—	Absorption heat transformer to distilled water
CO	—	Condenser
COP	—	Energy coefficient of performance, dimensionless
ECOP	—	Exergy coefficient of performance, dimensionless
EV	—	Evaporator
F	—	Factor of heat removal, dimensionless
GE	—	Generator
GTL	—	Gross temperature lift, °C
h	—	Enthalpy, kJ/kg
I	—	Total useful irradiation, kW/m^2
$\dot{m}$	—	Mass flow rate, kg/s
Q	—	Heat flow rate or power, kW
Q_u	—	Amount of useful energy extracted per area, kW/m^2
S	—	Incident solar radiation absorbed per area, W/m^2
SP	—	Solar panels
T	—	Temperature, °C

Greek letters

α	—	Absorbance of recipient, dimensionless
η	—	Efficiency, dimensionless
λ	—	Wavelength
τ	—	Transmittance of glass cover, dimensionless

Subscripts

a	_	Room temperature
c	_	Average temperature of absorbing plate
EXT	—	External
in	—	Inlet
out	—	Outlet
SP	—	Solar panels

References

[1] F.A. Peuser, K.-H. Remmers, M. Schnauss, Solar Thermal Systems: Successful Planning and Construction, Routledge Taylor & Francis Group, London, U.K., 2013.

[2] I. Horuz, B. Kurt, Absorption heat transformers and an industrial application, Renewable Energy, 35 (2010) 2175–2181.

[3] G. Jones, L. Bouamane, "Power from Sunshine": A Business History of Solar Energy, Harvard Business School, Working Paper Series, Cambridge, Massachusetts, U.S.A., 2012.

[4] C. Ramos-Berúmen, J.R. Ramírez-Benítez, J. Beltrán-Adán, Aplicaciones térmicas de la energía solar, en los sectores residencial, servicios e industrial (pág. 101), Instituto de Energías Renovables-Universidad Nacional Autónoma de México (IER-UNAM), Ciudad de México, 2017.

[5] S.S. Sahoo, S. Singh, R. Banerjee, Steady state hydrothermal analysis of the absorber tubes used in Linear Fresnel Reflector solar thermal system, Solar Energy, 87 (2013) 84–95.

[6] C. Xi, H.X. Yang, L. Lu, J.G. Wang, W. Liu, Experimental studies on a ground coupled heat pump with solar thermal collectors for space heating, Energy, 36 (2011) 5292–5300.

[7] L.M. Ayompe, A. Duffy, Analysis of the thermal performance of a solar water heating system with flat plate collectors in a temperate climate, Appl. Therm. Eng., 58 (2013) 447–454.

[8] Z. Said, R. Saidur, N.A. Rahim, M.A. Alim, Analyses of exergy efficiency and pumping power for a conventional flat-plate solar collector using SWCNTs based nanofluid, Energy Build., 78 (2014) 1–9.

[9] S.S. Meibodi, A. Kianifar, H. Niazmand, O. Mahian, S. Wongwises, Experimental investigation on the thermal efficiency and performance characteristics of a flat-plate solar collector using SiO_2/EG–water nanofluids, Int. Commun. Heat Mass Transfer, 65 (2015) 71–75.

[10] C. Koroneos, G. Roumbas, Geothermal waters heat integration for the desalination of sea water, Desal. Water Treat., 37 (2012) 69–76.

[11] N. Demesa, J.A. Hernández, J. Siqueiros, J.C. Garcia, A. Huicochea, Improvement of the performance of an absorption heat transformer through a single effect process to obtain freshwater, Appl. Therm. Eng., 78 (2015) 162–171.

[12] R.A. Huicochea, Puesta en marcha y evaluación experimental de un sistema portátil de purificación de agua integrado a un transformador de calor, Tesis de Maestría, Centro Nacional de Investigación y Desarrollo Tecnológico, México, 2004.

[13] D.T. Torres, Evaluación experimental de un transformador de calor utilizando Carrol-Agua, Tesis de Licenciatura, (CIICAP) Universidad Autónoma del Estado de Morelos, México, 2009.

[14] R.J. Romero, Estudio de las mezclas bromuro de litio – agua y CarrolTM – agua en transformadores de calor por absorción de una etapa, Tesis de Maestría, Laboratorio de Energía Solar, UNAM, México, 1996.

[15] R.M.B. Reyes, V.M.A. Gómez, A. García-Gutiérrez, Performance modelling of single and double absorption heat transformers, Curr. Appl. Phys., 10 (2010) S244–S248.

[16] W. Rivera, A. Huicochea, H. Martínez, J. Siqueiros, D. Juárez, E. Cadenas, Exergy analysis of an experimental heat transformer for water purification, Energy, 36 (2011) 320–327.

[17] R.J. Romero, W. Rivera, I. Pilatowsky, R. Best, Comparison of the modeling of a solar absorption system for simultaneous cooling and heating operating with an aqueous ternary hydroxide and with water/lithium bromide, Sol. Energy Mater. Sol. Cells, 70 (2001) 301–308.

[18] G.A. Florides, S.A. Kalogirou, S.A. Tassou, L.C. Wrobel, Design and construction of a LiBr–water absorption machine, Energy Convers. Manage., 44 (2003) 2483–2508.

[19] W. Rivera, R.J. Romero, Evaluation of a heat transformer powered by a solar pond, Sol. Energy Mater. Sol. Cells, 63 (2000) 413–422.

[20] F. Salata, M. Coppi, A first approach study on the desalination of sea water using heat transformers powered by solar ponds, Appl. Energy, 136 (2014) 611–618.

[21] L.B. Wang, X.B. Bu, H.Z. Wang, Z.T. Ma, W.B. Ma, H.S. Li, Thermoeconomic evaluation and optimization of LiBr-H_2O double absorption heat transformer driven by flat plate collector, Energy Convers. Manage., 162 (2018) 66–76.

[22] A.H. Hernández Soria, Estudio experimental de un sistema para purificación de agua acoplado a un transformador de

calor usando la mezcla carrol-agua, Tesis de Maestría, (CIICAP) Universidad Autónoma del Estado de Morelos, México, 2011.
[23] J.A. Manrique, Energía solar: fundamentos y aplicaciones fototérmicas (No. 621.47 M3), Ed. Harla, Mexico, 1984.
[24] H.W. Coleman, W.G. Steele Jr., Experimentation, Validation, and Uncertainty Analysis for Engineers, John Wiley & Sons, Inc., 2018.
[25] G.E. Dévora Isiordia, R. González Enríquez, S. Ruiz Cruz, Evaluation of desalination processes and their development in Mexico, Tecnología y Ciencias del Agua, 4 (2013) 27–46.
[26] CETENMA, Vigilancia tecnológica en energía y medio ambiente, Centro Tecnológico de la Energía y el Medio Ambiente, Sonora, Mexico, 2008. Available at: htpp://www.ctmedioambiente.es (accessed May 17, 2016).
[27] K.E. Herold, R. Radermacher, S.A. Klein, Absorption Chillers and Heat Pumps, CRC Press, Boca Raton, FL, U.S.A., 2016.
[28] C.C. Smith, T.A. Weiss, Design application of the Hottel-Whillier-Bliss equation, Solar Energy, 19 (1977) 109–113.
[29] R. Best, W. Rivera, M.J. Cardoso, R.J. Romero, F.A. Holland, Modelling of single-stage and advanced absorption heat transformers operating with the water/Carrol mixture, Appl. Therm. Eng., 17 (1997) 1111–1122.
[30] NOM 003-ENER-2011, Thermal Efficiency of Water Heaters for Domestic and Commercial Use, (Limits, Test Methods and Labeling that Provides a Methodology for Calculating the Solar System), Diario Oficial de la Federación, Tomo DCXCV, No. 7, Primera Sección, 28–43, August 9, 2011, Mexico City, Mexico, 2018.
[31] ASHRAE-93-1986/XAB, Method of Testing to Determine the Thermal Performance of Solar Collectors (ASHRAE Standard), American Society of Heating, Refrigerating and Air-Conditioning Engineers, Inc., Atlanta, GA (United States), 1986.
[32] REFPROP, Reference Fluid Thermodynamic and Transport Properties Database, National Institute of Standards and Technology (NIST), U.S. Department of Commerce, U.S.A., 2018.
[33] CONAGUA (Comisión Nacional del Agua; Data Provided by CONAGUA, May 23, 2017) Cuernavaca, Morelos, México.